Calculation of copper losses in case of Litz and twisted wires

2D Modeling and application for switched reluctance machine

Moustafa Al Eit, Fréderic Bouillault, Laurent Santandrea, Claude Marchand, Guillaume Krebs

GeePs|Group of electrical engineering - Paris
UMR CNRS 8507, CentraleSupélec, Univ Paris-Sud, UPMC Université Paris 6
3-11 rue Joliot-Curie, Plateau de Moulon, 91192 Gif-sur-Yvette Cedex
moustafa.aleit@supelec.fr

ABSTRACT. *The strong correlation between the level of eddy current losses and the winding geometry shows the necessity to pay attention to the manner of disposition of coils in machine slots. The conductor type, whether it is solid or stranded, also has a crucial influence. Since the transposition of winding strands reduces the degree of skin and proximity effects, it is a recommended solution to reduce eddy current losses. This article suggests an electromagnetic analysis of complex stranded conductors such as Litz and twisted wires. Each conductor is decomposed into individual strands that are twisted or woven in the slot throughout the length of the machine. Combined with several electric circuit relationships that interpret the transposition of the strands, a 2D finite element model is developed in this article so that the copper losses in each strand can be calculated individually.*

RÉSUMÉ. *La forte corrélation entre le niveau des pertes par courants de Foucault et la géométrie des enroulements montre la nécessité de porter une attention particulière sur la manière de disposer les spires dans l'encoche d'une machine et sur le type du conducteur utilisé s'il s'agit d'un conducteur massif ou d'un conducteur multi filamentaire. Puisque la transposition des filaments d'un conducteur réduit les effets de peau et de proximité, elle est recommandée comme solution pour diminuer les pertes par courants de Foucault. Cet article propose une analyse électromagnétique des conducteurs complexes tels que les fils de Litz et les fils torsadés. Chaque conducteur est décomposé en des filaments qui sont torsadés ou tressés entre eux au sein de l'encoche. Un modèle par éléments finis 2D, combiné à des relations de type circuit interprétant la transposition des filaments, est présenté dans cet article, il permet de calculer les pertes cuivre dans chaque fil individuellement.*

KEYWORDS: *finite element analysis, eddy currents, twisted wire, Litz wire, switched reluctance machine.*

MOTS-CLÉS : *analyse par éléments finis, courants de Foucault, fils torsadés, fils de Litz, machine à réluctance variable à double saillance.*

DOI:10.3166/EJEE.18.179-197

1. Introduction

The copper losses are subdivided into classical ohmic DC losses and additional eddy current losses. The latter exists due to the strong electromagnetic coupling between the current density and the time varying magnetic fields penetrating the copper conductors. Due to the fact that this interaction between electric and magnetic variables cannot be solved easily, then FE methods can be used to give a numerical solution.

Litz and twisted wires reduce eddy current losses in an effective way because of the strands transposition. The strands swap their positions in the slot throughout the length of the machine. Hence, because of their special geometry the 3D FE model is the suitable solution to pick up the electromagnetic effects. In spite of its precise solution, the 3D resolution leads to a substantial calculation time and requires large storage capacity. These heavy constraints hinder any process of design and optimization of winding geometries in terms of copper losses. Therefore, this article proposes a 2D FE model of such complex wires.

The test problem is the switched reluctance machine. This type of machine can be used in hybrid or electric vehicle where, for autonomy considerations, energy efficiency is crucial (Hannoun et *al.*, 2011). Multiple conductor types are studied such as solid, Litz wire and twisted wire conductors. By comparing the average copper losses over one cycle between different conductor types with the same filling factor and the same magnetomotive force waveform we will show the advantage of the strands transposition in reducing additional eddy current losses. Furthermore, numerous versions of stranded conductors with different number of strands and different geometry distribution of that strands in the conductor are analyzed in order to perform their influence on the additional eddy current losses.

2. Finite element method formulation

At low frequencies the displacement currents are neglected, then the Maxwell's equations in the electromagnetic domain Ω (Figure 1) of boundary Γ ($\Gamma = \Gamma_1 \cup \Gamma_2$ and $\Gamma_1 \cap \Gamma_2 = 0$) are given by:

$$\overrightarrow{curl}(\vec{H}) = \vec{J} \tag{1}$$

$$div(\vec{B}) = 0 \tag{2}$$

$$\overrightarrow{curl}(\vec{E}) = -\frac{\partial \vec{B}}{\partial t} \tag{3}$$

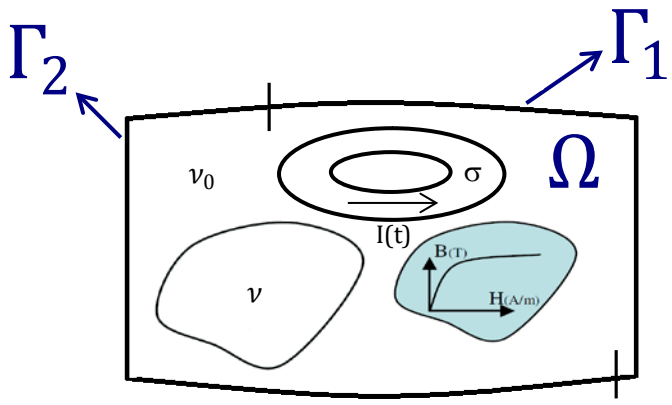

Figure 1. Non linear electromagnetic problem coupled with electrical circuits

Where $\vec{B}$ is the magnetic flux density vector, $\vec{H}$ is the magnetic field vector, $\vec{E}$ is the electric field vector and $\vec{J}$ is the current density vector. The associated constitutive medium relationships are:

$$\vec{H} = \nu \vec{B} \tag{4}$$

$$\vec{J} = \sigma \vec{E} \tag{5}$$

σ is the conductivity and ν is the reluctivity. ν_0 is the reluctivity of the air. For the ferromagnetic material with a non-linear behavior, ν may depend on the magnetic flux density B, then it is written as $\nu = \nu(B)$.

An easy coupling with the electrical circuits leads to use in a privileged way the potentials for example the magnetic vector potential $\vec{A}$ and the electric scalar potential V. From the Equation (2) the vector potential $\vec{A}$ is defined such that:

$$\vec{B} = \overrightarrow{curl}(\vec{A}) \tag{6}$$

To ensure the uniqueness of the solution, a gauge condition must be added. In our study we use the Coulomb's gauge:

$$div(\vec{A}) = 0 \tag{7}$$

And we impose the boundary conditions such that:

$$\vec{B}.\vec{n} = 0 \text{ on } \Gamma_1 \tag{8}$$

$$\vec{H}\Lambda\vec{n} = \vec{0} \text{ on } \Gamma_2 \tag{9}$$

Where $\vec{n}$ is the outward unit normal vector. According to the Equations (3) and (6) the electric scalar potential V is defined by the following equation:

$$\vec{E} = -\frac{\partial \vec{A}}{\partial t} - \overrightarrow{grad}(V) \tag{10}$$

The resultant Equation from (1), (4), (5), (6) and (10) is given by:

$$\overrightarrow{curl}(\nu \overrightarrow{curl}(\vec{A})) = -\sigma \frac{\partial \vec{A}}{\partial t} - \sigma \overrightarrow{grad}(V) \tag{11}$$

A combined circuit equation reflects that the current feeding the conductor of cross section S is $I(t)$:

$$I(t) = \iint_S \vec{J}.\overrightarrow{ds} = \iint_S (-\sigma \frac{\partial \vec{A}}{\partial t} - \sigma \overrightarrow{grad}(V)).\overrightarrow{ds} \tag{12}$$

In many electric machines where the conductors are placed longitudinally (in parallel to the z axis), the length of the machine is much higher than the transversal dimensions and the end effects can be neglected, the electromagnetic phenomena are supposed to be identical on each (x,y) plane normal to the z axis. The electromagnetic analysis may be simplified and then based on two dimensional finite element modeling of a single cross section of the investigated machine. The variational formulation of (11) through machine cross section with the 2D FE method as well as taking into account the circuit Equation (12) lead to the following matrix system (Piriou and Razek, 1988):

$$\begin{pmatrix} [S] + \dfrac{[T]}{\Delta t} & [D] \\ [D]^{\mathrm{t}} & \Delta t[G] \end{pmatrix} \begin{bmatrix} [A_t] \\ [\Delta V] \end{bmatrix} = \begin{bmatrix} \dfrac{[T]}{\Delta t}[A_{t-\Delta t}] \\ \Delta t[I(t)] + [D]^{\mathrm{t}}[A_{t-\Delta t}] \end{bmatrix} \tag{13}$$

ΔV is the electric potential drop per unit length and A_t is the z component of the magnetic vector potential at the instant t. Moving band technique is used to perform the rotor motion in the rotating machines, Newton-Raphson iterations are adopted to take into consideration the non linearity of the magnetic circuits and the backward Euler method is used for the time discretization.

3. 2D Modeling of Litz and twisted wires

We consider the case of a stranded conductor, placed in the slot of an electric machine. A SRM 8/6 is taken as an example. Half of the machine is modeled for reasons of symmetry and a simplified winding of 1 turn around the stator pole is studied. The turn conductor is composed of 9 parallel strands (Figure 2) that are insulated but electrically interconnected at the terminals.

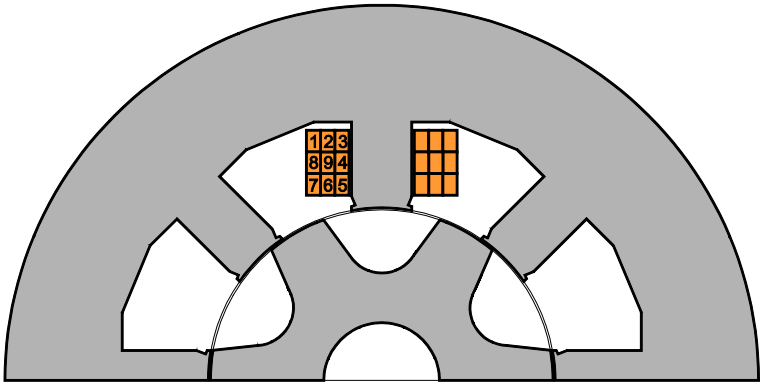

Figure 2. Position of the 9 parallel strands and the machine cross section

The control parameters of the current supply are precalculated by the software MRVSIM (Besbes and Multon, 2004). In our case, the winding is fed by the imposed current *I(t)* at the frequency of 710 Hz. Even though the strands are in parallel, the current *I*(*t*) is not equally distributed into the strands (Carstensen, 2007). The individual strand currents can be different as long as their sum is equal to the total current *I(t).* Figure 3 illustrates this phenomenon. In the magnetization period most of the coil current flows in the three lower strands (5, 6, and 7) located close to the air gap. In the demagnetization period the current of strand 5 becomes even negative although the total imposed coil current is positive. The distribution of the strands currents illustrates that the imposed current is displaced toward the air gap and that additional eddy currents circulate through the strands. The origin of the position axis in Figure 3 presents the unaligned position where the stator pole corresponding to the excited phase is equidistant from the two adjacent rotor poles as shown in Figure 2. The rotation from one unaligned position to the consecutive one corresponds to 360 electrical degrees.

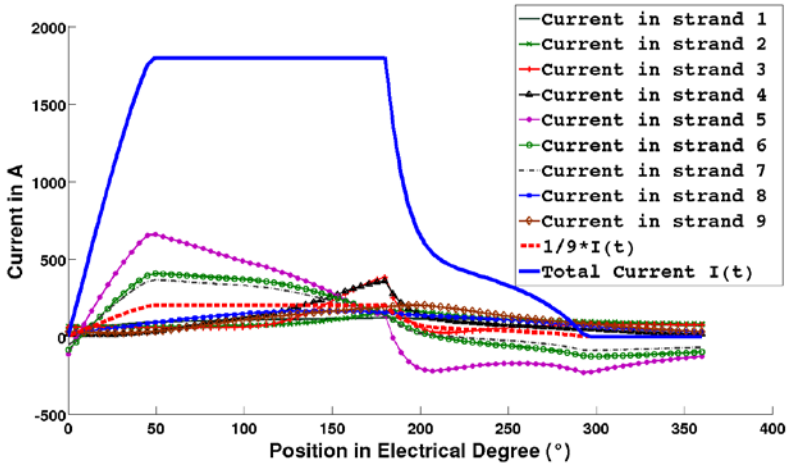

Figure 3. Unequal distribution of the total current into the 9 parallel strands

This asymmetric repartition of the current depends on the time varying magnetic fields penetrating the conductor in the winding slot; it's then a function of the strands positions relative to the magnetic circuit and the air gap. In a given point in the slot, the magnetic field varies either due to the time varying current (Sullivan, 1999) (skin and proximity effects) or to the stray flux caused by the salient rotor motion.

We consider now that a set of the conductor strands switch their positions in the slot throughout the length of the machine. If we start from the assumptions that the influence of the end windings is negligible and that the electromagnetic phenomena are identical on each section perpendicular to the longitudinal axis of the machine, then the transposed strands that occupy the same (x,y) positions successively will be subjected globally to the same electromagnetic effects. Due to the strong coupling between the current density and the time varying magnetic field the transposed strands will be governed by the same current density distribution. Taking into account this fact can be treated in a 2D FE model by enforcing the same current in each of the transposed strands (Howe, 1917; Lotfi and Lee, 1993; Carsten, 1986). The assumptions that the strands are in parallel and that the transposed ones are fed by the same current are added to system (13) in order to obtain a FE solution of the problem.

We take an example of a conductor divided into 4 parallel strands as shown in the Figure 4. The conductor is supposed located in the slot of an electric machine and fed by the current *I(t)*. As we mentioned before the current will be asymmetrically distributed into the strands.

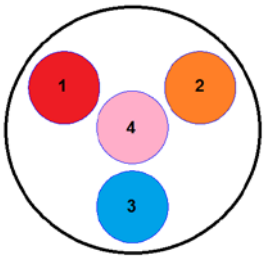

Figure 4. Cross section of the four parallel strands conductor

If the conductor is a twisted wire, then the strands 1, 2 and 3 will switch their positions every twisting pitch periodically while the central one will remain fixed. Sometimes, twisted wires are called bunched wires (Sullivan, 1999). We suppose that the twisting pitch has a length of Δl along the z axis. Figure 5 shows how the positions of the strands change throughout every periodic twisting pitch.

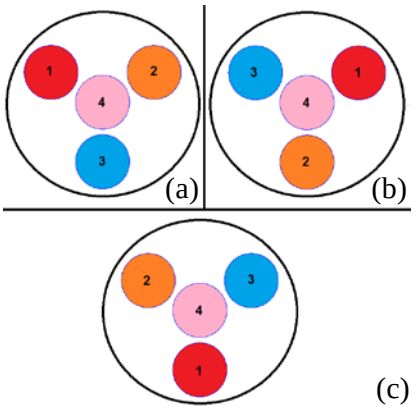

Figure 5. Strands positions throughout a twisting pitch with a length of Δl *along the z-axis. a)* $0 < z \le \frac{\Delta l}{3}$, *b)* $\frac{\Delta l}{3} < z \le 2\frac{\Delta l}{3}$, *c)* $2\frac{\Delta l}{3} < z \le \Delta l$

The disposition (a) of the strands in Figure 5 is only modeled by the FE method using the system (13) to which we associate the electric equations below that interpret the twisting of the parallel strands:

$$I_1(t) = I_2(t) \tag{14}$$

$$I_1(t) = I_3(t) \tag{15}$$

$$\Delta V_4(t) = \frac{\Delta V_1(t)}{3} + \frac{\Delta V_2(t)}{3} + \frac{\Delta V_3(t)}{3} \tag{16}$$

$$I_1(t) + I_2(t) + I_3(t) + I_4(t) = I(t) \tag{17}$$

Switching their positions, the strands 1, 2 and 3 will be fed by the same current as mentioned in Equations (14) and (15). We rely on the assumption that ΔV_i is the electric potential drop per unit length at the position of the strand i in the modeled cross section presented in Figure 5a.

Then, the strand 1 in its first position as shown in Figure 5a will be subjected to the electric potential drop $\Delta V_1 * \Delta l/3$. It will be subjected respectively to $\Delta V_2 * \Delta l/3$ at its second position (Figure 5b) and $\Delta V_3 * \Delta l/3$ at its third position (Figure 5c). The central strand 4, remaining fixed throughout the pitch length Δl, will be subjected to the electric potential drop $\Delta V_4 * \Delta l$. All strands are in parallel, for example strands 1 and 4, then they are covered by the same electric potential drop, hence the Equation (16). The Equation (17) shows that the sum of the strands currents is equal to total conductor current *I(t)*.

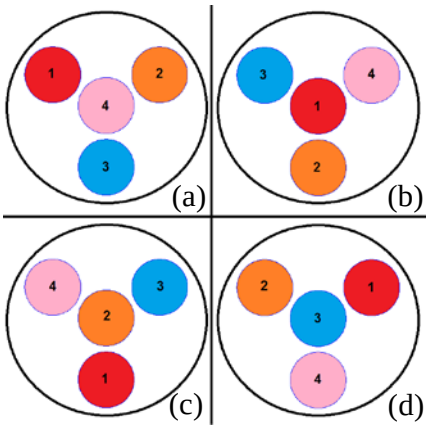

Figure 6. Strands positions throughout a weaving pitch with a length of Δl *along the z-axis. a)* $0 < z \le \frac{\Delta l}{4}$, *b)* $\frac{\Delta l}{4} < z \le \frac{\Delta l}{2}$, *c)* $\frac{\Delta l}{2} < z \le 3\frac{\Delta l}{4}$, *d)* $3\frac{\Delta l}{4} < z \le \Delta l$

In order to understand the 2D modeling methodology of the twisted wires, we have studied a very simplified example of a two-level twisted wire conductor. The first level consists of the central strand while the three peripheral strands present the second level. Actually the twisted wire conductor may be more complex and can involve several levels and even several groups of twisted wires that are, also in their

turn, twisted together. The study of other complex twisted wires can be done by following the same reasoning and applying the same principles mentioned in the electric circuit equations already cited.

Though in case of Litz wire, all the strands switch their positions every weaving pitch periodically. We suppose that the weaving pitch has a length of Δl along the z axis. Figure 6 shows an example of how the positions of the strands may change throughout every periodic weaving pitch.

In case of LW, all the strands occupy the same positions consecutively as shown in Figure 6. They will be subjected globally to the same electromagnetic effects and will be fed hence by the same current *I(t)/4*. Only one disposition of the strands for example that of Figure 6a is modeled using the system (13) to which we associate the electric equation below that interprets the transposition of all strands :

$$I_1(t) = I_2(t) \tag{18}$$

$$I_1(t) = I_3(t) \tag{19}$$

$$I_1(t) = I_4(t) \tag{20}$$

$$I_1(t) + I_2(t) + I_3(t) + I_4(t) = I(t) \tag{21}$$

In fact, as reminded by Bartoli *et al.* (1996), Tang and Sullivan (2003), the DC resistance of a transposed stranded conductor is larger than that of a solid conductor with the same length and equivalent cross-sectional area. That is because the distance a strand travels when it alternates its position is longer than when it goes straight. However, in this article we consider them equal to better focus on the effect of the strand transposition on the reduction of additional eddy current losses. Nevertheless, a more accurate calculation of a strand copper losses is given by:

$$P_{copper} = P_{2DF.E} * \frac{lr}{\Delta l} \tag{22}$$

l_r is the real length of the strand along the stranded conductor twisting or weaving pitch Δl. P_{copper} is the more authentic copper losses in that strand taking into account the increasing in its length due to the conductor strands transposition. $P_{2DF.E}$ is the copper losses calculated by the 2D finite element proposed model considering Δl as the uniform length of all strands. The increasing in length factor $l_r \diagup \Delta l$ may vary from one strand to another due to their different trajectories along the twisting pitch within the same stranded conductor and from one wire type to another due to the different techniques used in the transposition of the conductor strands.

4. Application examples

The implementation of the 2D modeling approach of Litz and twisted wires is performed on a 2D finite element model of a switched reluctance machine 8/6. Half of the machine is studied for periodic reasons and only one phase is fed. Initially, a simplified winding is studied. It consists of two coils connected in series; each of them has 1 turn. Each coil is placed on a stator pole. The turn is either a solid conductor of surface *S* and a filling factor η or a stranded conductor of the same surface and the same filling factor. The stranded conductor can be a Litz wire or a twisted wire. It is composed out of *p* parallel strands insulated but electrically interconnected at the terminals. Several numbers of strands are studied for both Litz and twisted wire, for example 25, 36, 64 and 81 to show at the same filling factor the influence of the number of conductor strands on the eddy current losses. First, we investigated the solid conductor winding. It has a cross section with a height of 13mm and a width of 8.5mm. At the electric frequency of *f*=710Hz, the skin depth of the fundamental is equal to 2.54 mm. The solid conductors are placed in the machine slots with a filling factor η of 26.9%.

Both the copper losses of the left coil side and those of the right coil side for one electrical period are presented in Figure 7. At constant speed the rotor position is proportional to time. The losses are plotted as a function of rotor position, because electrical degrees are more intuitive than a time scale. The loss curves for the back and forth conductors are not identical since these two conductors are subjected to different magnetic stray fields during the rotor motion. We admit that the rotor moves in the counter clockwise. The right coil side or the forth conductor is the one in the proximity to which the rotor passes at the magnetization period.

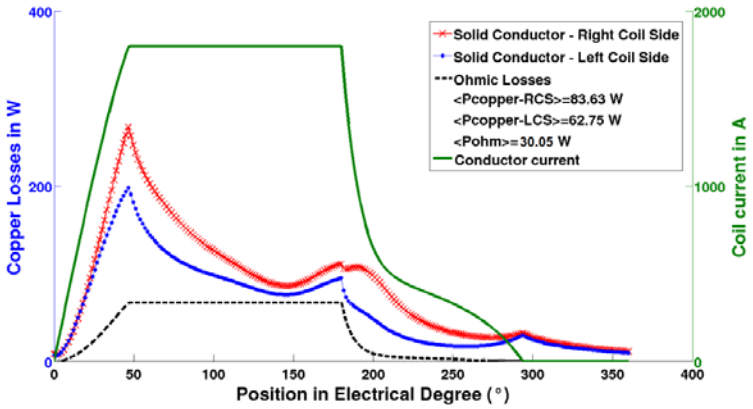

Figure 7. Copper losses in the right coil side and in the left one in case of solid conductor

The highest losses occur during the magnetization period. In the period in which the current is kept constant the losses decay and approach the curve of the DC losses, which defines the smallest possible loss value. At the instance the supply current disappears, there are still coil losses present. The current densities don't disappear instantly but eddy currents continue to circulate in the coil even though the supply current is null. In Figure 8 the cross sections of the back and forth solid conductors are each divided into 81 portions in the post processing in order to show the spatial distribution of the mean copper losses. The bars show the spatial average of the copper losses of each solid conductor portion.

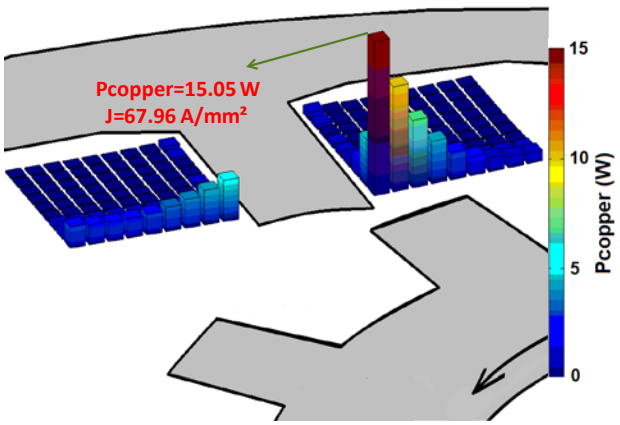

Figure 8. Spatial distribution of the mean copper losses in case of solid conductor

The losses are not uniformly distributed, they increase from the slot bottom toward the airgap, and they achieved their highest values in the portions which are located closest to the air gap right next to the stator pole (Klauz and Dorrell, 2006). In the right coil side the time varying stray flux due to rotor motion causes additional eddy current losses, hence the predominance of the copper losses on that side. The uniform spatial average of the DC ohmic losses is 0.37W. It corresponds to a DC current density of 8.43A/mm². The maximum power losses of 15.05W in the right coil side potion located closest to the air gap corresponds to a current density of 69.76A/mm². These values are far too high for conventional cooling methods.

Secondly, we investigated the stranded conductor winding configuration. It is similar to the solid conductor winding in terms of the cross section surface and the filling factor. They are also fed by the same magnetomotive force waveform. The difference is that each turn conductor is a stranded conductor; it is composed out of p parallel strands. In the first place, we treated the case without the strands transposition. The copper losses calculation has shown that the solid conductor division into parallel strands without transposition is not sufficient to reduce the

additional eddy current losses. It allows having roughly equal losses on both coil sides while the overall mean copper losses have undergone a very slight reduction. In the second place, these parallel strands are transposed in the form of Litz and twisted wires. As we mentioned before, several values of *p* are studied for both Litz and twisted wires. These values are 25, 36, 64 and 81. Figure 9 shows an example of how the stranded conductors with a number of strands *p* of 25 are placed in the machine slots.

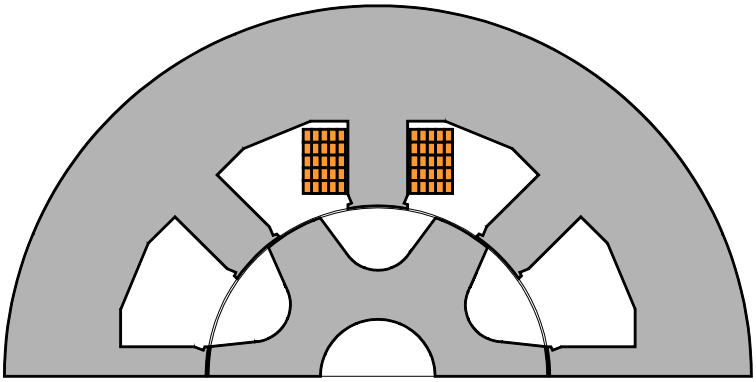

Figure 9. Geometry distribution of the 25 parallel strands and machine cross section

The copper losses of twisted and Litz wires as a function of rotor angle are presented respectively in Figure 10 and Figure 11. Compared to the solid conductor winding, the losses in case of Litz and twisted wire winding are significantly reduced. They decay much faster during the freewheeling periods. They reach lower maximum values and also drop to the level of the DC ohmic losses in both cases for an interval of time during the constant current periods. This interval of time is larger in case of Litz wires. The copper losses are almost equal to zero in both Litz and twisted wire cases when the conductor current disappears.

The comparison between the copper losses curves in both Litz and twisted wires cases for different number of strands shows the advantage of the subdivision of the solid conductor into strands and the transposition of that strands. Table 1 shows the values of the mean copper losses of one electric period for the different winding geometries. These values accentuate the positive influence of the transposition in reducing the power losses. The higher is the number of strands the less are the additional eddy current losses. We must note that, in real applications, with fine stranding, the eddy current losses can be decreased, but DC losses increase as a result of the space occupied by insulation (Sullivan, 1999).

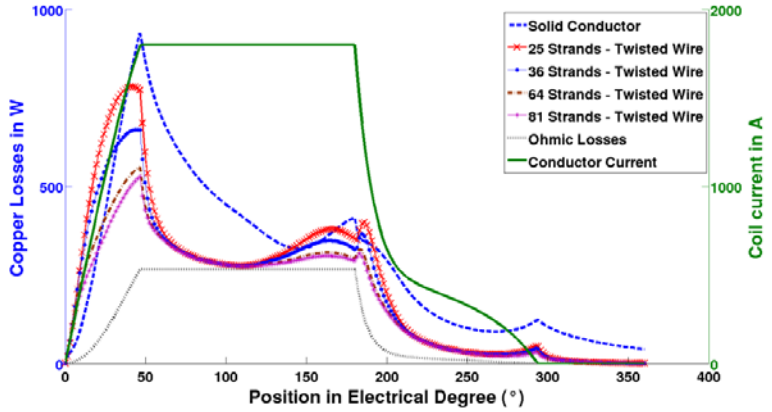

Figure 10. Copper losses in case of twisted wire conductor for multiple numbers of strands

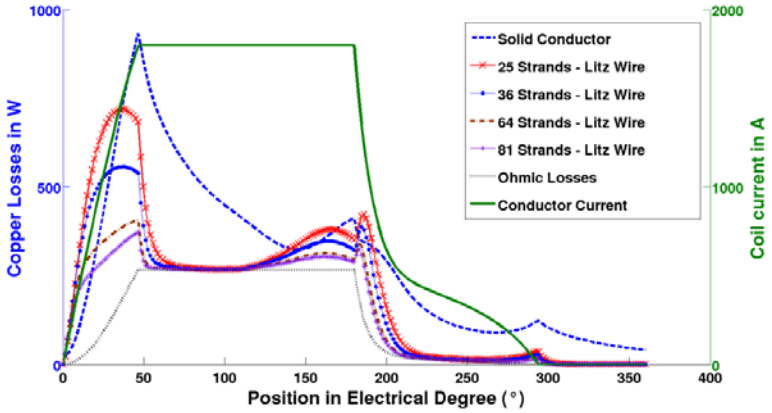

Figure 11. Copper losses in case of Litz wire conductor for multiple numbers of strands

As we can see from Table 1, both Litz and twisted wires reduce considerably the additional eddy current losses with a slight precedence of Litz wires. Twisting the strands, being the cheapest between the strands transposition techniques, might be a better compromise between losses reduction and price. Nevertheless, to go further in reducing losses the Litz technique is more adequate.

Table 1. Mean copper losses of the different winding geometries in comparison to DC losses

Number of Strands	Copper Losses (W)			DC Ohmic Losses (W)
	Twisted wire	Litz Wire	Solid Conductor	
25	228,9	211,9	295,6	120.2
36	209,8	188,2		
64	188,5	161,1		
81	181,4	152,9		

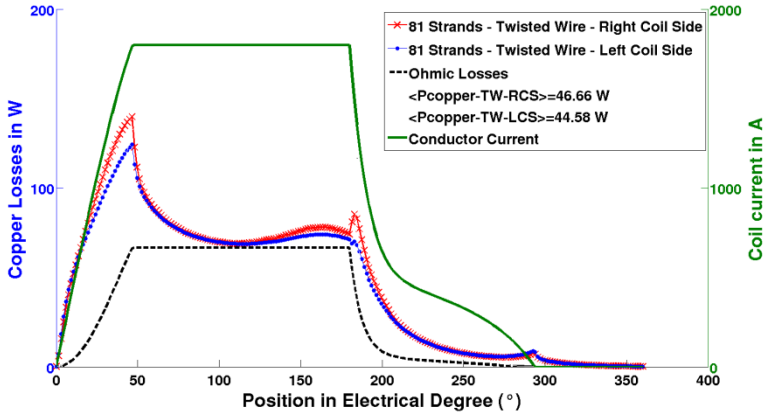

Figure 12. Copper losses in the right coil side and in the left one in case of 81 strands twisted wire conductor

Figure 12 presents both the losses of the right coil side and the left coil side of the 81 strands twisted wire geometry. Unlike to the solid conductor geometry these two curves are closer to one another; the mean copper losses for one electric period are almost the same.

Furthermore, the spatial distribution of the mean copper losses is plotted in Figure 13. The losses are uniform on each group of transposed strands. The losses in both coil sides are almost equal and hence the influence of the rotor stray flux on the left coil side is almost negligible. This is due to the parallel strands configuration throughout the coil which balances the current density distribution on the both coil sides.

The peripheral conductors, switching their positions, become for a period of their slot path close to the air gap, hence their highest value of copper losses. The maximum mean power loss of 0.78 W in the peripheral conductor of the right coil

side corresponds to a current density of 14.27 A/mm². The spatial loss distribution is much more uniform compared to the solid conductor winding. Furthermore the peak values of power losses and current densities are moderated which is a benefit regarding hot spot temperature reduction.

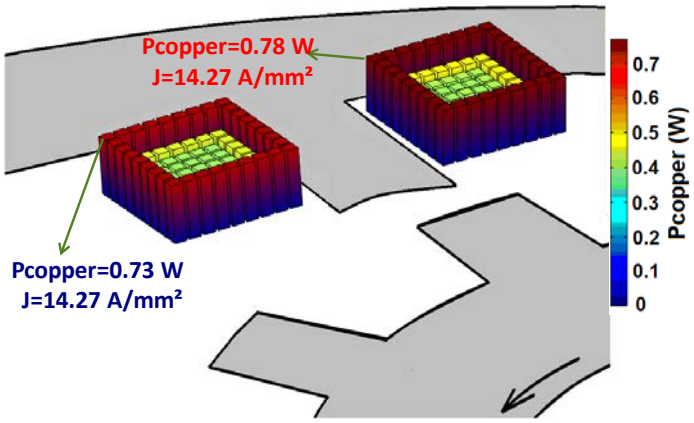

Figure 13. Spatial distribution of the mean copper losses in case of 81 strands twisted wire conductor

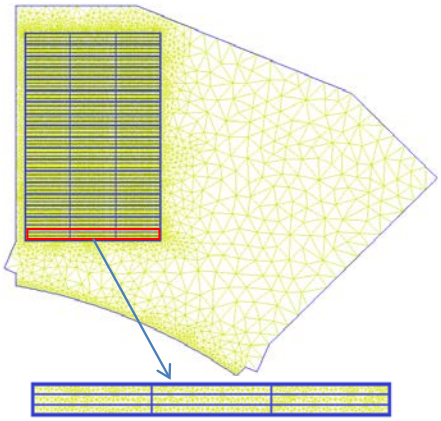

Figure 14. Geometry configuration of the 18 horizontal turns-Each conductor is a 9 stands Litz wire

A second study is carried out on a more realistic winding consisting of numerous turns per pole. Only one phase is fed. It consists of two coils connected in series. Each coil is placed on a stator pole; it has 18 turns that are wound horizontally or vertically as two examples. The filling factor is η and the coil is always fed by the

same magnetomotive force waveform. In the case of horizontal turns two winding geometries are studied. In the first geometry, the turn conductor is a solid conductor of surface *s=S/18*. In the second geometry, the turn conductor, of the same surface *s*, is a Litz wire which is composed out of 9 strands (3x3) as showed in the Figure 14.

The comparison between the copper losses in the cases of the solid conductor and the Litz wire conductor shows the advantage of such wires to reduce the eddy current losses and the range of variation of the current densities. The use of the Litz wire conductors instead of solid conductors led to a reduction of 20% of the copper losses (Figure 15).

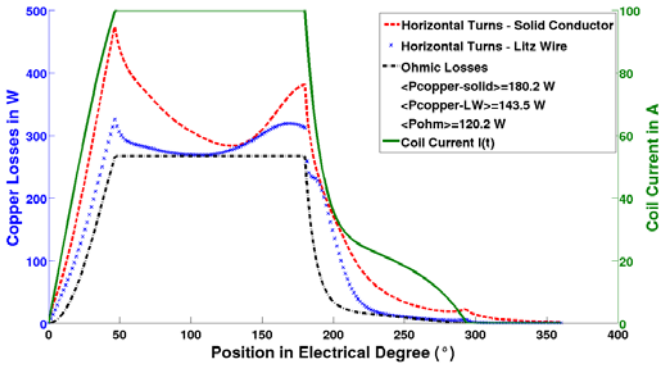

Figure 15. Copper losses in case of solid horizontal turns and Litz wire horizontal turns

In case of solid conductor horizontal turns, the right coil side turn placed in proximity to the air gap has a wide range of variation of the instantaneous current densities. These values range between -169 and 70 A/mm². This corresponds to the rotor position angle 48° where the losses present their maximum (Figure 15), this range of variation is reduced in case of Litz wire conductor, it is between -65 and 25 A/mm² (Figure 16). Subdivision and transposition thus avoided excessive instantaneous values of the current density.

In the case of vertical turns, the use of a first version of the Litz wire turns (3x3), as shown in Figure 17, led unexpectedly to an elevation of the mean copper losses (Figure 18).

The choice of a second version of Litz wire which is composed out of 9 strands (9x1) placed vertically (Figure 19) led in the opposite of the first version to a reduction of 45% of the copper losses (Figure 20) which accentuates the importance of the geometry of distribution of the conductor strands beside the importance of the number of strands on the reduction of the additional eddy current losses.

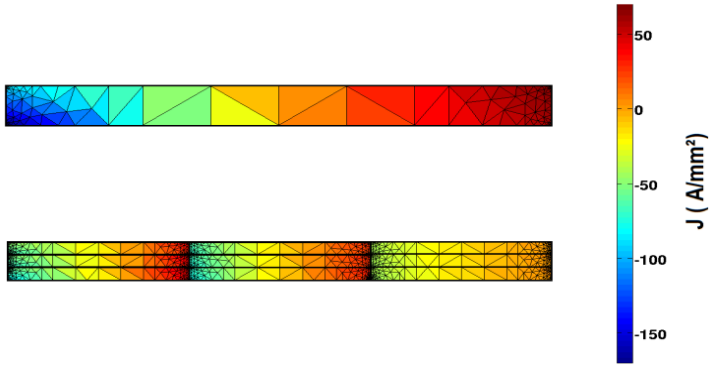

Figure 16. Current density distribution in the solid horizontal conductor close to the air gap in the right coil side (up), Litz wire conductor (down) (Position=48°)

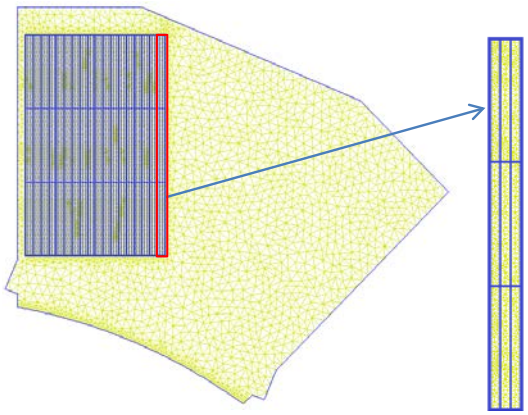

Figure 17. Geometry configuration 18 vertical turns-Each conductor is a 9 stands Litz wire (Version 1)

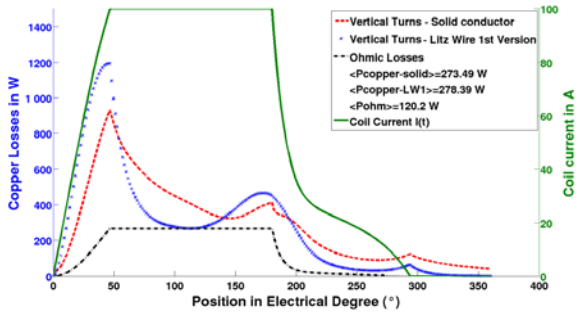

Figure 18. Copper losses in case of solid vertical turns and Litz wire vertical turns (Version 1)

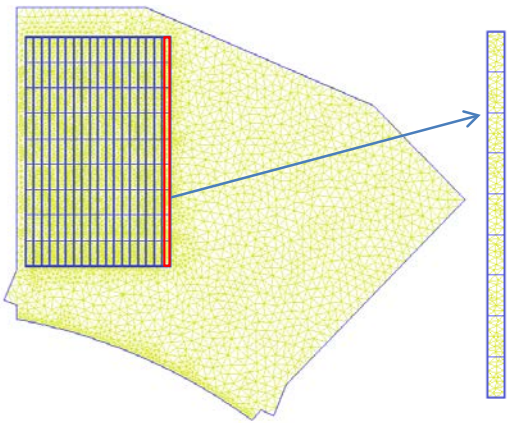

Figure 19. Geometry configuration 18 vertical turns-Each conductor is a 9 stands Litz wire (Version 2)

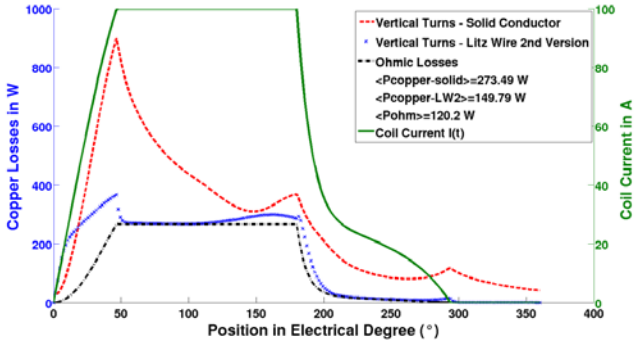

Figure 20. Copper losses in case of solid vertical turns and Litz wire vertical turns (Version 2)

5. Conclusion

The 2D FE method used to model complex winding geometries such as twisted and Litz wires has verified the interest of these windings in reducing additional eddy current losses. We have pointed out the high influence of the number of strands and of their geometry of distribution in the conductor on the power losses. When it prevents the 3D FE model, the 2D modeling reduces the calculation time and the required storage capacity. Practically, the stranded conductors will not show their advantage compared to solid conductor unless they decrease the copper losses in a factor much higher than that of the increasing of the classical DC losses. The increasing of the DC losses takes place due to the transposition of the strands and hence due to the increasing of their length compared to the length of a solid conductor that goes straight.

This 2D modeling approach of such complex winding geometries allows precise and fast calculation of the current densities and the copper losses in each wire individually. When it is associated with a reduced model of the machine, it can be used in many optimization problems when we search the optimized geometry distribution and the optimized achievable number of strands for a given machine winding.

Bibliography

Bartoli M., Noferi N., Reatti A., Kazimierczuk M.K. (1996). Modeling Litz-wire winding losses in high-frequency power inductors. *In 27th Annu. IEEE Power Electronics Specialists Conf.*, vol. 2, p. 1690-1696.

Besbes M., Multon B. (2004). *MRVSIM Logiciel de simulation et d'aide à la conception de Machines à réluctance variable à double saillance à alimentation électronique*. Deposit APP CNRS, 2004, IDDN.FR.001.430010.000.S.C.2004.000.30645.

Carsten B. (1986). *High frequency conductor losses in switchmode magnetic*. In Tech. Papers of the *1st Int. High Frequency Power Conversion 1986 Conf.*, p. 155-176.

Carstensen C. (2007). *Eddy Currents in Windings of Switched Reluctance Machines.* PhD Thesis in engineering and sciences, RWTH Aachen University.

Hannoun H., Hilairet M., Marchand C. (2011). Experimental validation of a switched reluctance machine operating in continuous-conduction mode. *IEEE Trans. On Vehicular technology,* vol. 60, n° 4, p. 1453-1460.

Howe G.W.O. (1917). The High-Frequency Resistance of Multiply-Stranded Insulated Wire. *Proceedings of the Royal Society of London. Series A, Containing Papers of a Mathematical and Physical Character*, vol. 93, p. 468-492.

Klauz M., Dorrell D.G. (2006). Eddy current effects in a switched reluctance motor. *IEEE Trans. On Magnetics*, vol. 42, n° 10, p. 3437-3439.

Lotfi W., Lee F.C. (1993). A high frequency model for Litz wire for switch-mode magnetics. *In Conf. Rec. 1993 IEEE Industry Applications Conf. 28th IAS Annu. Meeting*, vol. 2, p. 1169-1175.

Piriou F., Razek A. (1988). Coupling of saturated electromagnetic systems to non linear power electronic device. *IEEE Trans. On Magnetics*, vol. 24, n° 1, p. 274-277.

Sullivan C.R (1999). Optimal Choice for Number of Strands in a Litz-Wire Transformer Winding. *IEEE Trans. On Power Electronis*, vol. 14, n° 2, p. 283-291.

Tang X., Sullivan C.R. (2003). Stranded wire with uninsulated strands as a low cost alternative to Litz wire. *IEEE Power Electronics Specialist Conference 34th Annual*, vol. 1, p. 298-295.

Received: 29/07/2015
Accepted: 3/11/2015